Dark and sunlight-driven dye degradation over a TiO$_2$–dibenzoylmethane hybrid xerogel

Claudio Imparato [a,*], Manfred Maria Bonifazzi [a], Gerardino D'Errico [b], Aurelio Bifulco [a], Olimpia Tammaro [c], Serena Esposito [c], Antonio Aronne [a], Domenico Pirozzi [a,*]

[a] Department of Chemical, Materials and Production Engineering, Università di Napoli Federico II, P.le Tecchio 80, 80125 Naples, Italy
[b] Department of Chemical Sciences, Università di Napoli Federico II, Via Cinthia, 80126 Naples, Italy
[c] Department of Applied Science and Technology and INSTM Unit of Torino - Politecnico, Politecnico di Torino, Corso Duca degli Abruzzi 24, 10129 Turin, Italy

HIGHLIGHTS

- TiO$_2$-dibenzoylmethane hybrid catalysts are produced by a sol-gel route.
- The ligand-to-metal charge transfer complexes activate visible light response.
- The complexes induce the formation of stable superoxide radicals at the surface.
- Methylene blue removal from water is achieved both under sunlight and in the dark.
- Solar light improves the oxidative degradation rate and the reuse stability.

GRAPHICAL ABSTRACT
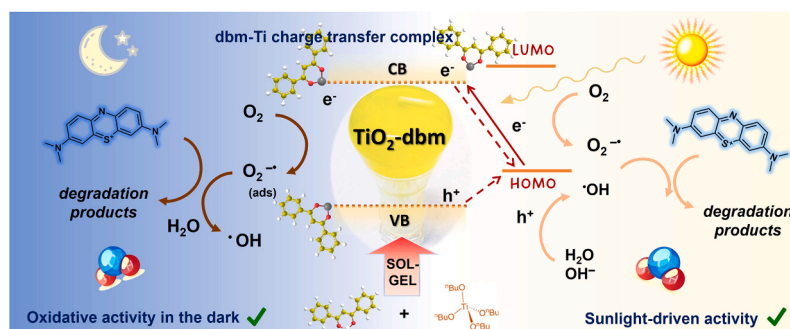
ARTICLE INFO

ABSTRACT

The pursuit of sustainable and inexpensive systems for the degradation of organic aquatic pollutants working under sunlight or even without irradiation is still open. Herein, an amorphous titanium oxide modified with dibenzoylmethane, an aromatic diketone, is proposed as a solar photocatalyst showing oxidative activity also in the dark. Ti(IV)-dibenzoylmethanate (dbm) complexes form during the sol-gel synthesis and are dispersed throughout the oxide gel structure. This ligand-to-metal charge transfer complex plays a dual role: it enables visible light absorption, narrowing the apparent band gap, and provides localized surface charge, promoting the spontaneous formation and stabilization of superoxide radical ions by reduction of O$_2$. The activity of the TiO$_2$-dbm hybrid was assessed in the removal of methylene blue from aqueous solution. The results demonstrated a rather stable photocatalytic activity under natural sunlight, exceeding 80% dye removal after 1 h in four subsequent tests, a value that was mostly recovered after a mild regeneration. Considerable efficiencies were also achieved in the dark, owing to the immobilized superoxide radicals acting as initiators of degradation pathways. Finally, the influence of the operating conditions (pH, illumination, mixing method, water contact) on the efficiency and durability of the performances was evaluated to survey the long-term utilization in water decontamination. The behaviour of this hybrid material resembles a "photocatalytic memory" effect and may widen the perspectives for the development of heterogeneous advanced oxidation processes.

1. Introduction

Water pollution represents a major concern for ecosystems and human health. The contaminants contained in industrial and municipal wastewaters, such as dyes, pharmaceuticals, pesticides, detergents, and heavy metal ions, are often water-soluble, therefore they can diffuse not only in the superficial water bodies but also in the groundwater, seriously affecting the water quality. Many of these xenobiotic compounds are toxic and an increasing number is regarded as endocrine disruptor or carcinogenic [1–3]. Their persistence in water bodies threatens aquatic organisms and poses the risk of their entry into the food chain. The organic and inorganic dyes, discharged mainly by textile industries, are known to be responsible for up to 20% of anthropogenic pollution [4]. Beyond their variable toxicity, dyes prevent the penetration of sunlight into the water and their gradual oxidative decomposition reduces the concentration of dissolved oxygen, negatively affecting photosynthesis, aquatic life, and the self-purification capacity of natural waters [1]. The study of dye adsorption or removal attracts interest also for their use as a proxy for other compounds more difficult to track, e.g. per- and polyfluoroalkyl substances (PFAS) [5]. The conventional treatments to remove dyes and other organic pollutants include ultrasonication, ozonation, coagulation, and nanofiltration. These methods are limited by different bottlenecks, associated with the high energy requirements, the high operation and maintenance costs, and the generation of secondary pollutants [6]. Adsorption offers an alternative [7], however it only transfers pollutants between different phases. Advanced oxidation processes based on the production of reactive oxygen species appear to be the most promising solutions for environment and health protection, particularly for the purification and disinfection of water and air, aiming at the transformation of the contaminants into less harmful compounds. These technologies usually rely on semiconducting materials such as metal oxides, which work either through a photocatalytic mechanism, consisting in the generation of ROS following photoexcitation, or through the activation of ROS sources, such as peroxides (Fenton and Fenton-like process) or peroxymonosulfate [8–10]. There is a huge research interest in the modification of TiO_2 and other semiconducting oxides to make them responsive not only to UV radiation but also to visible light, so as to exploit a broader fraction of the solar spectrum, possibly avoiding the use of UV lamps [11]. Doping TiO_2 with metals and nonmetals and its photosensitization with dye compounds have been widely studied to this end [12,13], sometimes with contrasting outcomes [14]. Alternatively, the sensitization by ligand-to-metal charge transfer complexes involving small organic molecules is a less known, yet promising approach [15,16]. An even more convenient and ecofriendly solution is the development of materials able to initiate oxidation processes without a continuous light exposure or a radical initiator. Such systems would reduce the consumption of energy and chemicals, overcoming the constraints in the design of photoreactors or at least improving the performances under discontinuous radiation sources (such as solar light) [17–20]. Hence the recent interest in "round the clock" photocatalysts, showing a catalytic memory after the illumination [21,22]. In this scope, we have discovered that hybrid materials based on titanium or zirconium coordinated with acetylacetone (Hacac) exhibit the unusual ability to generate superoxide radical ions in ambient conditions and immobilize them for long times [23–25]. This special property enabled the degradation of different organic pollutants in the dark, aided by the formation of hydroxyl radicals in water solution [25,26]. The stability of the superoxide radicals on these solids is due to the role of the ligands, which form charge transfer complexes with the metal and stabilize the excess charge at the defective oxide surface, as corroborated by theoretical models [27]. Additionally, these complexes originate a visible light absorption band, and, consequently, TiO_2-acac materials also showed an enhanced photocatalytic activity [28,29]. Intriguingly, the functionalization of metal-organic frameworks based on Zr, Ti, Cr, or Al with Hacac was reported to promote the formation of singlet oxygen even with indoor lighting [30].

These promising results urged us to design improved materials that could extend the efficiency and applicability of this kind of system, seeking material compositions that ensure a higher yield of oxygen radicals, a better stability in the working environment (water solution), possibly using only safe chemicals (Hacac has non-negligible toxicity and was found to be gradually released upon prolonged contact of TiO_2-acac with water [25]). Moreover, there are open questions regarding the functionality of these hybrid materials, for example the possible contribution of light irradiation in their activity and reuse. In this work, dibenzoylmethane (1,3-diphenyl-1,3-propanedione, Hdbm), an aromatic β-diketone, was selected as the organic ligand. This molecule is found in the root extracts of licorice and is not considered harmful to humans and the environment [31]. Its tautomeric keno-enol equilibrium, shown in Scheme 1, is largely shifted toward the enol form, providing it with extended conjugation and excellent chelating ability toward various metals [32]. Rare earth complexes of its deprotonated form, i.e. dibenzoylmethanate (dbm), have applications related to their luminescence properties [33], while derivatives, such as avobenzone, are used in sunscreen formulations owing to their UV absorption. Surprisingly, there are very few reports in the literature about the interaction of Hdbm with metal oxides, besides some studies about photosensitive ZrO_2 films for the fabrication of diffraction gratings [34] and the influence of the metal complex in TiO_2-based layers on a photopolymerization reaction [35]. We recently prepared by sol-gel titanium oxide-dbm thin films [36] and powders [27], and found for the latter an increased efficiency in the adsorption and reduction of O_2 to superoxide radicals compared to TiO_2-acac, in agreement with density functional theory (DFT) calculations. Owing to its molecular structure, coordinated dbm can provide a large electron delocalization and change the surface properties of the material, for example making it more hydrophobic [37]. Here, we synthesized a series of TiO_2-dbm nanostructured hybrid materials with multiple aims: 1) obtaining chemical gels rather than precipitates, thus allowing better control of the structure and granulometry; 2) exploring the influence of the organic ligand content on the properties; 3) testing the activity and stability of these new materials in the degradation of a model pollutant without illumination; 4) assessing the effect of solar light and other operating parameters on their performance. The xerogels prepared at low temperature were characterized to assess their main structural and physicochemical properties. Then the activity of the selected sample was validated in the removal of methylene blue, an extensively used and potentially harmful cationic dye, from aqueous solution, both in the dark and under natural sunlight. Moreover, the effects of solution pH and mixing speed on the decolourization efficiency in the batch system were evaluated. The results evidenced that TiO_2-dbm has a better removal activity than the reference TiO_2 and that a direct photocatalytic contribution by solar light greatly improves the removal rate and prolongs the reusability.

2. Experimental

2.1. Sol-gel synthesis

TiO_2-dibenzoylmethanate (TiO_2-dbm) hybrid materials were prepared by a hydrolytic sol-gel route, using titanium (IV) n-butoxide (97%) and dibenzoylmethane (1,3-diphenyl-1,3-propanedione, Hdbm, 98%) as precursors, 1-propanol (99.8%) and cyclohexane (99.5%) as solvents and hydrochloric acid (37%) as catalyst, all purchased by Sigma-Aldrich. The procedure was addressed to produce chemical gels instead of precipitates. Different amounts of Hdbm were dissolved in a mixture of cyclohexane and 1-propanol (2.4:1 v/v), in a sufficient solvent volume to allow its complete dissolution (about 30 mg/mL). This solution was added to Ti(IV) n-butoxide, and the mixture was stirred for 30 min. A hydrolytic solution, containing HCl diluted in deionized water (0.1 mol/L), cyclohexane, and 1-propanol (1:0.6:1.2 v/v) was then gradually added to the first one, and the system was left under stirring at

room temperature until gelation. The obtained transparent yellow gels were aged for 2 days and then dried at 50 °C in a ventilated oven. The granular xerogels were ground before characterization. The samples prepared with a dbm/Ti molar ratio equal to 0.05, 0.10, and 0.20 are named T-dbm005, T-dbm01, and T-dbm02, respectively.

2.2. Characterization of the materials

X-ray diffraction (XRD) measurements were performed using a Philips X'PERT-PRO diffractometer (Philips, Netherlands) with monochromatized CuKα radiation (40 mA, 40 kV) at a step width of 0.013° 2Θ. Fourier Transform infrared (FTIR) spectra were recorded using a Nicolet 5700 FTIR spectrometer (Thermo Fisher, Waltham, MA, USA), equipped with a DTGS KBr (deuterated triglycine sulfate with potassium bromide windows) detector. The transmittance spectra were acquired by mixing the sample in KBr pellets, collecting 32 scans with a resolution of 2 cm^{-1}. Thermogravimetric and differential thermal analysis (TGA-DTA) were performed by a SDT Q600 simultaneous thermoanalyser (TA Instruments, New Castle, DE, USA), heating in nitrogen at 10 °C/min rate. Diffuse reflectance ultraviolet-visible (DRUV–vis) spectra were recorded on a Shimadzu UV-2600i double beam spectrophotometer (Shimadzu, Kyoto, Japan) with an ISR-2600Plus two-detector integrating sphere. The samples were dispersed in BaSO$_4$, used as blank. The band gap energy values were estimated by the Tauc plot method. Electron paramagnetic resonance (EPR) spectra were acquired on the solids using an X-band (9 GHz) Bruker Elexys E-500 spectrometer (Bruker, Rheinstetten, Germany). The capillary containing the powder was placed in a 4 mm quartz sample tube. For each sample, 16 scans were collected at room temperature with the following settings: sweep width, 140 G; resolution, 1024 points; modulation frequency, 100 kHz; modulation amplitude, 1.0 G; time constant, 20.5 ms; attenuation, 10 dB. The g-factor values and the spin densities were evaluated by means of an internal standard, Mn^{2+}-doped MgO, and calibrated with reference to a diphenylpicrylhydrazyl (DPPH) standard solution. Zeta-potential (ζ-potential) data were obtained by measuring the electrophoretic mobility as a function of pH at 25 °C by means of electrophoretic light scattering (ELS) with Litesizer (Anton Paar Instruments, Worcestershire, UK). The samples were prepared with a starting concentration of 1 mg/100 mL, and subsequently, the pH was gradually adjusted by the addition of either 0.1 M NaOH or 0.1 M HCl. The ζ-potential measurements were carried out in an Omega cuvette (Anton Paar) accessory. The measurements were performed in triplicate. To verify the stability of the hybrid material in water, samples were kept under stirring in deionized water for 30 min, then separated, dried, and subjected to the same washing step, up to three times. After each cycle, the supernatant was analyzed by UV–vis spectrometry and after the third cycle, FTIR spectra were recorded on the recovered powders.

2.3. Methylene blue removal tests

Sunlight-driven photocatalysis experiments were conducted in October 2022 in Naples, Italy (40° 51' N, 14° 14' E) with an average solar irradiance of 320 W/m^2 and an average daytime temperature of 22 °C. The degradation of methylene blue (MB) was generally carried out by using T-dbm02 powders (the most promising sample based on characterization results) at a solid/liquid ratio R= 10 g/L for different incubation times (usually 60 min) in a MB solution at the initial concentration of 0.050 g/L. The suspension was kept in an orbital shaker (40 rpm) and the system was either exposed to solar light around midday in sunny weather or shielded from light (dark experiments). The tests were performed at pH values between 5 and 9. At fixed times, 2 mL samples were taken, the liquid phase was separated by centrifugation, and the residual MB concentration was measured spectrophotometrically (λ = 660 nm). The experimental curves of MB concentration as a function of the exposure time could be described by adopting a first-order kinetic model:

$$\ln \frac{C}{C_0} = -k \cdot t \qquad (1)$$

where C is the MB concentration after a given exposure time t, C_0 is the initial concentration and k is the pseudo-first order rate constant (min^{-1}).

2.3.1. Repeated batches

The repeated batch tests were carried out keeping the samples under the same conditions previously described. After each cycle, the photocatalyst was collected by centrifugation, washed with deionized water, and dried overnight, then the test was repeated.

2.3.2. Regeneration of the catalyst

After a cycle of 7 repeated batches, the photocatalyst was collected by centrifugation and washed with deionized water. After washing in water, the samples were kept 96 h in a ventilated oven, ensuring full contact with air. Tests were conducted to shed light on the performance of the photocatalyst towards MB degradation before and after the regeneration process.

2.3.3. Long-term stability of the catalyst

Long-term stability tests were carried out keeping photocatalyst samples in the aqueous solution at pH 9 and exposing them to solar light for longer periods to simulate the conditions of a real application. The experiments were carried out by adopting two different mixing techniques of the suspension: an orbital shaker, at a relatively slow mixing speed (40 rpm); and a flask with a magnetic stirrer at a faster mixing speed (200 rpm). Periodically (every 2 days on average), the photocatalyst was collected by centrifugation, and then used to carry out a MB
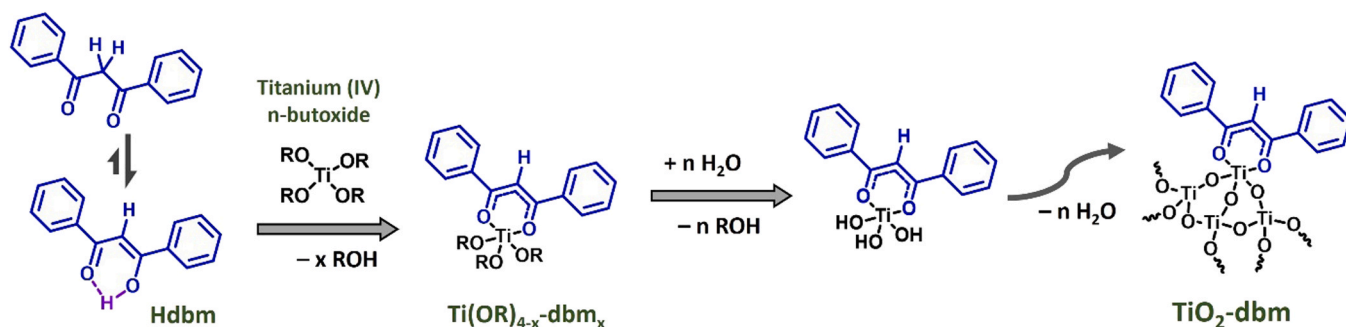
Scheme 1. Synthesis of TiO$_2$-dbm hybrid material: molecular structures of the keto and enol form of dibenzoylmethane (Hdbm) and proposed structure of a heteroleptic complex formed by the reaction of a titanium(IV) alkoxide, Ti(OR)$_4$ (where R = Bu in case of Ti(IV) n-butoxide), with the deprotonated form, dibenzoylmethanate (dbm); schematic illustration of hydrolysis and condensation reactions, the successive steps in the sol-gel synthesis of dbm-modified titania.

degradation test as previously described. After each test, the photocatalyst was regained by centrifugation to continue the long-term exposure to solar light.

3. Results and discussion

3.1. Synthesis of the hybrid materials

TiO$_2$-dbm materials were prepared via a bottom-up sol-gel route that allows the production of inorganic-organic structures with defined stoichiometry and high homogeneity under mild operating conditions. The process starts with the formation of Ti(IV)-dbm complexes in solution. Dibenzoylmethane easily reacts with Ti(IV) n-butoxide precursor, replacing a butoxide group, so that a fraction of the Ti(IV) ions are involved in heteroleptic coordination complexes, Ti(OR)$_{4-x}$·dbm$_x$, as illustrated in a simplified way in Scheme 1. Then, upon addition of the aqueous solution, hydrolysis and condensation reactions simultaneously occur. In the hydrolysis, the oxygen of a water molecule attacks Ti(IV), inserting a hydroxyl group in place of an alkoxide and producing an alcohol molecule. This step is catalyzed by an acid that protonates the leaving groups (here a small amount of HCl was used). In the condensation, the oxygen of a hydroxyl or alkoxide group forms a bridge between two metal centers, originating Ti-O-Ti bonds [38,39]. Condensation reactions and aggregation of primary particles lead to the growth of the Ti-O-Ti network, finally resulting in an amorphous titanium oxide matrix with part of Ti(IV) ions coordinated by dbm. Such an approach allows a uniform distribution of the organic ligands, linked to the metal ions through strong coordination bonds. The interactions of Ti(IV) alkoxides with several complexing organic molecules, including β-diketones, have been widely explored in sol-gel chemistry since the resulting oxo oligomers show variable stability and reactivity and can be used as nano building blocks in the synthesis of hybrid materials [39–41]. For example, in the case of zirconium alkoxides, it was reported that partial Hdbm substitution reduces the condensation rate more than Hacac, which was attributed to the bulkier structure of the ligand, exposed on the surface of the growing particles [42]. According to a successive general interpretation of the sol-gel transition, this latter is governed by the aggregation of oligomers, acting as "micelles templated by self-assembly of ligands", rather than further hydrolysis and condensation [43]. This process was confirmed to be strongly dependent on the chemical nature of both ligand and solvent [44]. In 1-propanol the Ti-dbm sols, bearing exposed phenyl rings, formed precipitates after the addition of water [27]. Conversely, the introduction of cyclohexane, lowering the medium polarity with respect to pure propanol, improved the affinity between solvent and ligand and then the dispersion of the surface-functionalized oligomers. This promoted the formation of homogeneous chemical gels, even at the lowest dbm/Ti ratio, confirming the effectiveness of dbm as stabilizing ligand, likely related to the steric hindrance and nonpolar exposed groups. The gelation times for the three samples increased with the complexing ratio, from about one minute (T-dbm005) to a few hours (T-dbm02), in agreement with the role of the ligand in modulating the growth rate of the three-dimensional network.

3.2. Physicochemical properties

The structural and chemical features of the hybrid xerogels were studied by XRD, FTIR, and thermal analysis. A representative XRD pattern (Fig. S1) shows that the samples have an essentially amorphous nature, as commonly found in gels dried at low temperature. The FTIR spectra of pure dibenzoylmethane and the hybrid samples are displayed in Fig. 1. Due to the prevalent enol form of Hdbm in the solid state, stabilized by the formation of an intramolecular hydrogen bond, no evidence of C=O groups is seen in the 1600–1800 cm^{-1} region [45]. The lack of such bands in the spectra of the hybrids supports the expected coordination of dbm as enolate. As a consequence, most of the dbm
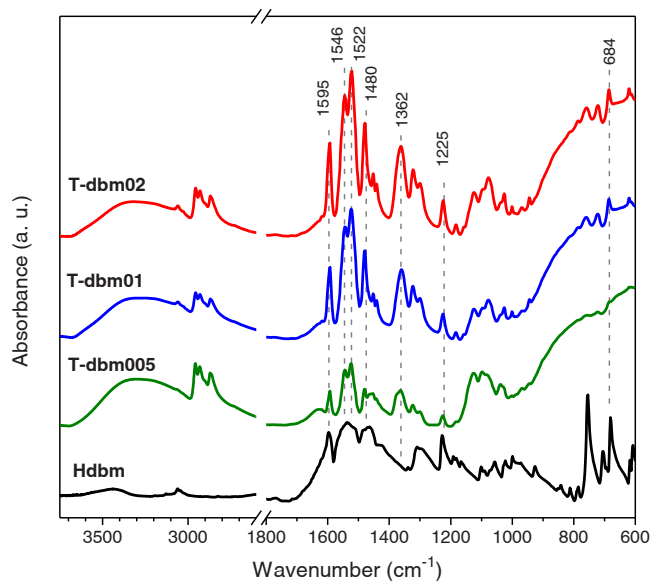

Fig. 1. FTIR spectra of pure dibenzoylmethane and the Ti-based hybrid samples. The intensities of the latter spectra are normalized with respect to the band of Ti-O stretching, centred around 600 cm^{-1}.

vibrations are not noticeably shifted with respect to the pure molecule. The spectra match those recorded on TiO$_2$-dbm films and powders [27, 36]. Thus, the bands between 1595 and 1480 cm^{-1} can be assigned to symmetric and asymmetric stretching vibrations of C-O bonds involved in the coordination, some of them being combined with vibration modes of the phenyl ring [46]. It can be noted that the intensity of the bands due to the organic ligand tends to increase relative to the Ti-O stretching band (the broad feature below 900 cm^{-1}) with the increase of dbm/Ti nominal ratio. The band appearing in the hybrid samples at 1362 cm^{-1} follows the same trend, sustaining its attribution to the Ti-dbm complex. Consistent with the FTIR spectra, a bidentate chelating coordination occurs, which is the most thermodynamically favoured binding mode according to DFT modelling of a dbm-modified TiO$_2$ surface [27]. The presence of Ti-OH groups is attested by the broad O-H stretching band around 3300 cm^{-1}. The bands in the ranges 2800–3000 and 1000–1200 cm^{-1} are associated with residual alkoxide groups and organic solvent molecules (mainly 1-propanol) trapped in the gel structure after the low-temperature drying (50 °C).

At the prospect of using the materials in water decontamination, the stability of their hybrid structure in an aqueous medium was tested by repeated washing, as detailed in the Experimental. After each contact with water, the supernatant was analysed by UV–vis spectroscopy to check the possible release of the organic component in the liquid phase. The results for T-dbm02 (Fig. S2) show the appearance of a rather weak absorption band centred at 230–240 nm, whose intensity decreases upon consequent washing stages, becoming very low after the third one. That band cannot be attributed to Hdbm, as the molecule has an absorption centred around 336 nm, nor to the alcohols and cyclohexane, which do not absorb above 200 nm, thus a possible explanation is the occurrence of a partial self-oxidation of dbm, forming small amounts of a by-product, for example, benzoic acid [47]. To prove that this possible phenomenon is marginal and does not significantly affect the organic ligand, FTIR spectra were recorded after the third washing (Fig. S3). The signal appeared almost unaltered, except for the disappearance of the abovesaid solvent-related bands, with only a slight reduction in the relative intensity between the peaks of dbm and the one linked to the oxide matrix. Similar results were confirmed for the other two samples, attesting a good resistance of the Ti-dbm complex complex to hydrolysis, whose strength is related the electron delocalization of chelated dbm in the enolate form.

Thermogravimetric and differential thermal analysis (TG-DTA) was carried out to further examine the composition of the hybrid materials and assess their thermal stability. The TGA curves of the three TiO$_2$-dbm xerogels are displayed in Fig. 2a. Their mass loss occurs in three main steps. The first, in the range of 50 – 200 °C, is due to the volatilization of adsorbed water and solvent molecules. The major and steepest mass loss event, around 21 wt% for all samples, with an inflection point at about 280 °C, is associated with an endothermic DTA peak (Fig. 2b) and corresponds to the thermal degradation of most of the organic phase, consisting in dbm and a fraction of non-hydrolyzed alkoxide. Finally, the third mass loss, which increases with the nominal ligand content (see Table S1), takes place from about 350 °C to 450 °C in T-dbm005 or up to 520 °C in the other two samples and is likely related to the pyrolysis of carbonaceous residues [24,48]. To confirm this interpretation, FTIR spectra on the T-dbm01 sample heated in nitrogen up to 240 and 300 °C were recorded (Fig. S4). The former reflects the spectrum of the as prepared gel, confirming the thermal stability of Ti-dbm complexes, whereas the latter shows clear modifications, with the disappearance of some bands related to the complex, indicating that between 240 and 300 °C the decomposition of the ligand occurs. Even if the overall mass losses are comparable, the thermal profiles suggest that the dbm content in the samples actually approaches the nominal values (corresponding to 9, 18, and 36 wt% for T-dbm005, T-dbm01, and T-dbm02, respectively). The larger overall mass loss of T-dbm005 compared to T-dbm01 can be explained by a larger content of adsorbed water, residual solvent molecules and alkoxide ligands retained in the formed sample. Indeed, T-dbm005 shows the highest mass loss below 200 °C (see also Table S1). This observation agrees with FTIR spectra, as the features due to the solvent and alkoxide the appear relatively more intense for T-dbm005 than T-dbm01 (Fig. 1). The crystallization of the amorphous matrix, evidenced by exothermic DTA peaks, occurs as soon as the removal of organic components is completed, hence shifting from about 400 °C for T-dbm005 to 480–500 °C for the other two materials.

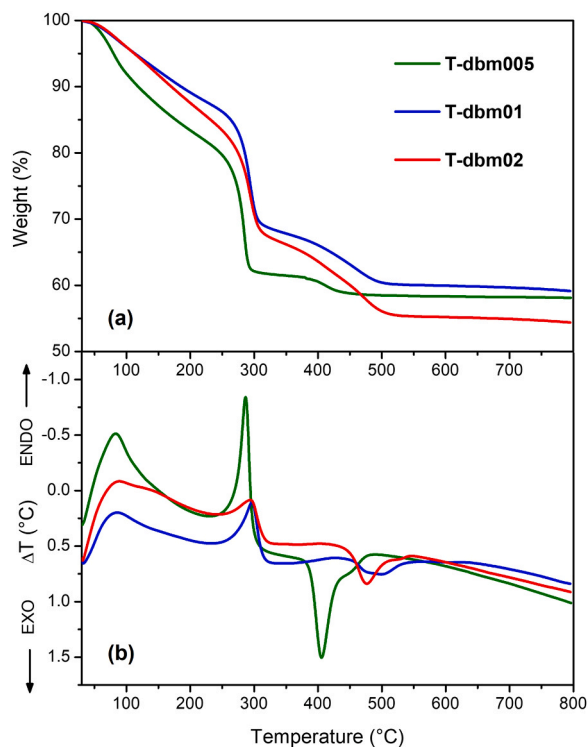The optical properties of the hybrid materials were evaluated by means of DR UV–vis spectroscopy (Fig. 3). Beside the typical absorption band of titanium oxide in the UV range [49], an additional band, centred at about 395 nm with a tail reaching 480–500 nm, is evident in all samples. Hdbm absorbs mainly UV light, with a maximum at 340 nm attributed to π-π* transitions [50], therefore the new feature, whose intensity grows with the dbm content, demonstrates the occurrence of a ligand-to-metal charge transfer (LMCT) between dbm and titanium. It can be described as a partial transfer of electron density from the HOMO of the bonded molecule to the Ti 3d orbitals composing the conduction band of the oxide. This observation is in agreement with the previously studied gel-derived TiO$_2$-dbm materials and with the DFT calculations on this system [27]. The apparent band gap energy resulting from the additional electronic transition, estimated by Tauc plot elaboration considering an indirect gap (see Fig. S5), is about 2.6 eV. The DRUV–vis spectra confirm that the TiO$_2$-dbm powders can absorb a fraction of visible light, consistent with their bright yellow colour (see the inset in Fig. 3), owing to the LMCT complex providing photosensitization.

The ability of the TiO$_2$-dbm hybrid xerogels to produce and immobilize radicals was examined by EPR spectroscopy. All the spectra (Fig. 4), acquired at room temperature without any pre-treatment of the powders, show the typical lineshape and g-factor values of the superoxide anion radical ($O_2^{\bullet-}$) adsorbed on the TiO$_2$ surface. Similar EPR spectra were observed after contact with H$_2$O$_2$ and/or photoirradiation on TiO$_2$ as well as other Ti^{4+}-containing materials, like titanium silicalite TS-1 [51,52] and SrTiO$_3$ [53], or dysprosium-doped TiO$_2$ modified with salicylic acid [54]. Anyway, in these works neither long-term stability of the radicals nor oxidative activity without irradiation were reported. The three g values that characterize the recorded signal correspond to those of TiO$_2$-acac samples, indicating that the $O_2^{\bullet-}$ radicals are localized on similar surface sites [25]. It can be seen that the intensity of the signals clearly increases with the dbm/Ti ratio. The relative spin concentrations, namely the density of radical species, are estimated to be about $1.1 \bullet 10^{16}$, $1.9 \bullet 10^{16}$, and $2.7 \bullet 10^{16}$ spin/g for T-dbm005, T-dbm01 and T-dbm02, respectively. These values are about one order of magnitude larger than the one found for TiO$_2$-acac materials, confirming the superior efficiency of dbm in the generation and stabilization of superoxide radicals [27]. Along with the increase of radical density with the dbm content, these results point to the fundamental role played by the charge transfer complex and by the charge delocalization related to the molecular structure of dbm in the reduction of adsorbed O$_2$.

The presence of the superoxide radicals was monitored in time by repeating the EPR measurements after storing the powders for different times in test tubes in the lab. After about one year the EPR signals were still visible, although with lowered intensity. The decrease was found

Fig. 2. (a) TGA and (b) DTA curves of the hybrid materials recorded in a nitrogen atmosphere.
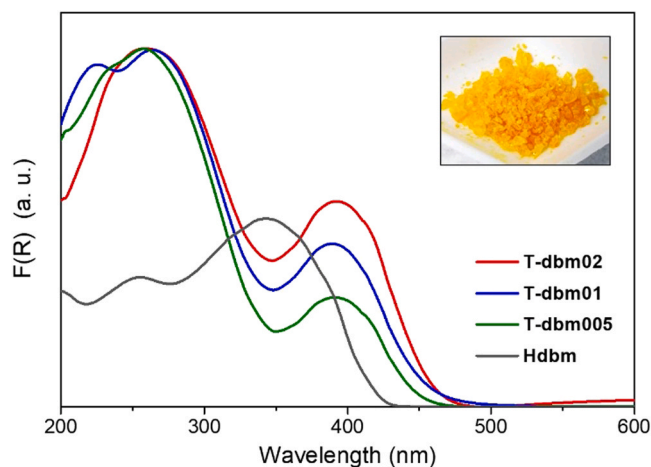

Fig. 3. DRUV–vis spectra of the hybrid samples and pure dibenzoylmethane, reported as the normalized Kubelka-Munk function of reflectance. In the inset, the picture of a T-dbm02 xerogel is shown.
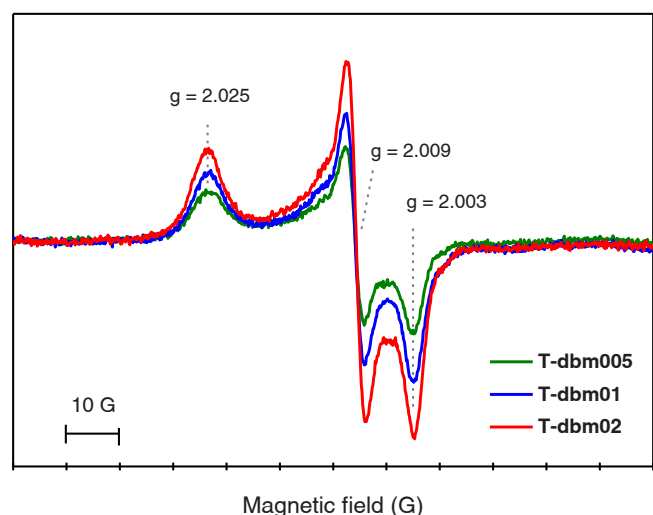
Fig. 4. EPR spectra of the TiO$_2$-dbm hybrid samples, recorded in the air at room temperature.

Fig. 5. Effect of pH on the sunlight-mediated removal of MB after 60 min in the presence of TiO$_2$-dbm and P25-TiO$_2$.

more significant for T-dbm005 and T-dbm01 than for T-dbm02. In the latter sample, the signal was clearly detectable also after 2 years of storage, as shown in Fig. S6. This result attests to the outstanding ability of this hybrid material to preserve reactive oxygen species on its surface, in line with previous findings on the TiO$_2$-acac system [25]. The immobilization of O$_2^{\bullet-}$ radicals was demonstrated to enable the materials to degrade organic pollutants [24,25] and even to support anticancer therapy, as reported for ZrO$_2$ nanoparticles modified with acac and hyaluronic acid [55]. Ultimately, T-dbm02 proved to be the sample providing the highest yield and stability of superoxide radicals and showing at the same time the most intense visible light absorption, as both these properties are related to the concentration of Ti-dbm complexes. Therefore, this hybrid material composition was selected for the investigation of the degradation activity in aqueous solution.

3.3. Removal of methylene blue dye from water

Owing to its extensive use as a dyestuff in textile industries, methylene blue (MB) was chosen as a model compound to carry out the removal tests. MB can exert toxicity on aquatic life and cause potential adverse effects and dermatological diseases in humans [56]. The removal tests were carried out in batch systems using T-dbm02 and commercial TiO$_2$ (P25) as reference material, investigating the effect of different operating conditions, namely pH, sunlight radiation, contact time, and stirring, on the decolourization of the solution.

3.3.1. Effect of pH

MB is a cationic dye and its interaction and reactivity with solids are known to be influenced by pH [57]. For this reason, the first series of experiments was performed to individuate the optimal pH for its removal. Fig. 5 displays the results collected by keeping the suspension in an orbital shaker (40 rpm), under sunlight radiation, at a pH ranging from 5 to 9. Both TiO$_2$-dbm and P25-TiO$_2$ could remove a considerable fraction of MB in 1 h. In all cases, the removal percentage obtained with the hybrid sample was higher in comparison to that observed with P25. The removal efficiency was significantly dependent on pH, as the amount of disappeared dye increased with pH, following a similar trend for both materials.

The variation of pH affects the charge distribution of both the dye and the titania particles. MB is mainly found in its undissociated form (MB^0) in an acidic solution, whereas its cationic form (MB$^+$) predominates in the neutral and basic environment [58]. The effects of the ligand (dbm) on the surface charge of TiO$_2$-based materials were
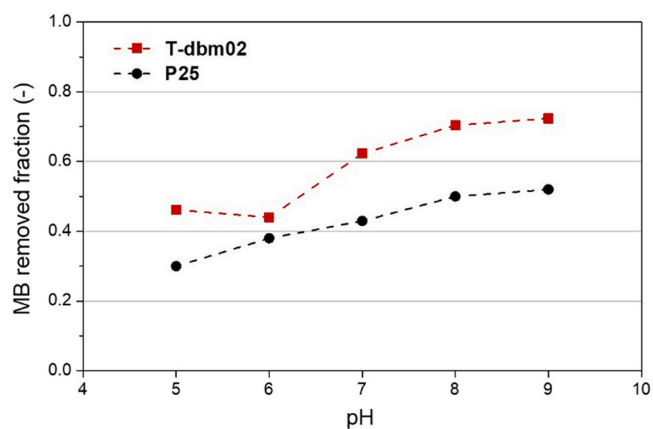
evaluated by measuring the surface zeta (ζ) potential of T-dbm02 and P25 as a function of pH, as reported in Fig. 6. The surface charge of hydrous oxides is influenced by the presence of the "charge determining ions" (H$^+$ and OH$^-$), hence by the acidity of the established hydroxyl groups. Therefore, when pH < PZC (point of zero charge) the surface is positively charged, while in the case of pH > PZC it is negatively charged. Fig. 6 shows that the ζ-potential curve of P25 is coherent with the behaviour reported in the literature, with a PZC of about 7 [59–61]. The presence of dbm in the hybrid structure shifts the PZC value of T-dbm02 towards a lower pH value (about 4.5). The overall result is a negatively charged surface over a wider pH range, compared to the bare titania. This behaviour is reflected in a higher affinity, due to electrostatic attraction, between the dye (MB$^+$) and the hybrid sample, compared to MB$^+$ and P25. Further experiments to assess the effects of other process parameters were performed keeping a pH value of 9.0, being the removal of MB more efficient under alkaline conditions. However, it is worth noting that at pH 8 the efficiency is very close to that observed at pH 9, also in repeated cycles (see Section 3.3.3), indicating that the material can be effective also in a system not far from real environmental conditions, as the pH of natural freshwater is often slightly alkaline, depending on the dissolved species, temperature and other variables [62].
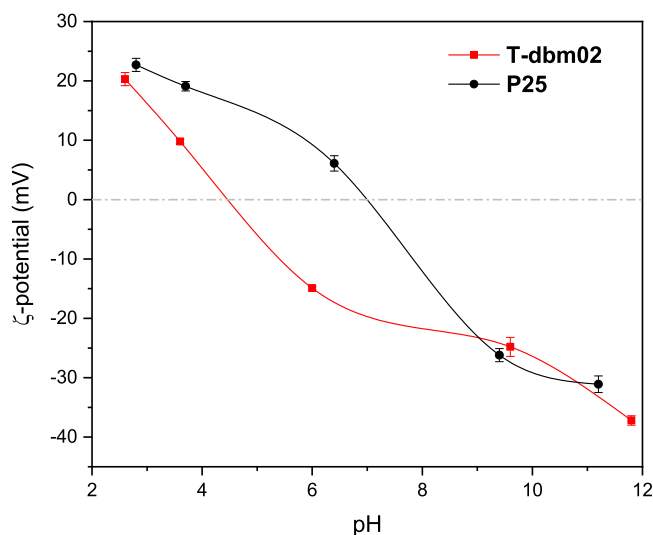

Fig. 6. Zeta potential of synthetized T-dbm02 (square red line). The zeta-pot curve of P25-TiO$_2$ (circle black line) is also reported as reference material.

3.3.2. Effect of sunlight exposure

To understand the effect of light on the dye removal mechanism, experiments were conducted under natural sunlight and in the dark. As reported in Fig. 7a, the results indicate that under sunlight exposure, T-dbm02 leads to a higher MB removal (up to 98% after 2.5 h) than in the dark. In the control photolysis test, no MB degradation was observed under sunlight radiation in the absence of a catalyst (data not shown). Therefore, the hybrid material can be considered as a photocatalyst active in the degradation of MB under solar radiation. Again, the obtained removal fraction was higher than that recorded with P25 TiO$_2$: for example, after 1 h, the percentage of removed dye was 73% for T-dbm02 and 52% for P25. The relatively good activity of the latter is probably due to the portion of UV radiation contained in the solar spectrum. P25 TiO$_2$ does not usually show photocatalytic activity under visible light, however, it is known to be highly efficient under UV irradiation, which can lead to the degradation rate observed in the adopted experimental conditions.

It is important to remark that the hybrid titania showed significant efficiency also when the tests were performed in the dark. As a matter of fact, about 56% of the MB was removed in 2 h in the presence of T-dbm02, whereas the dye concentration was almost unchanged in the presence of P25 (Fig. 7a). The occurrence of a chemical transformation of MB rather than its simple surface adsorption also in the absence of light, suggested by the combination of EPR and zeta potential analysis (vide supra), is also supported by the results of repeated removal experiments (see Section 3.3.3). After each batch test, the water used to wash the catalyst has been analysed for the concentration of MB released. The amount of MB released was in any case less than 1% of the amount removed from the liquid solution during the previous batch test. This result is inconsistent with the hypothesis of adsorption equilibrium and suggests that a negligible fraction of MB is removed by pure adsorption.

The trends of the experimental data in Fig. 7a were reasonably described by adopting a first-order kinetic model (Eq. 1 in the Experimental), showing a correlation coefficient higher than 0.88. The corresponding values of the apparent first-order rate constants are reported in Table 1. It can be observed that the first-order rate constant (k) of T-dbm02 is 62% higher than that of P25. Comparable rate constants were reported for the photodegradation of MB over a large number of TiO$_2$-based heterostructures [4]. Representative results from publications about the degradation of MB under sunlight or visible light using modified TiO$_2$ (doped, metal-loaded, coupled with other semiconductors, sensitizing dyes or carbon materials) are summarized in Table S2. It is worth noting that the removal rate constant in the absence of light is still almost one third of the value found under sunlight. Because of the activity of TiO$_2$-dbm in the dark, in contrast to conventional photocatalytic materials, here the relative contribution of adsorption and chemical degradation on the decay of MB concentration are difficult to distinguish, so the apparent rate constants are referred to both phenomena that likely occur simultaneously. In the case of TiO$_2$-acac particles embedded in a PVP-silica electrospun mat, a similar MB concentration decay in the dark was better fitted by a modified pseudo-first order model [63], possibly because of the contribution of the SiO$_2$ nanoparticles to the adsorption step.

3.3.3. Long-term stability and regeneration of the hybrid material

To assess the activity and stability of TiO$_2$-dbm under long-term operation and cycling, two sets of experimental tests were performed. The first consisted of repeated batches lasting 1 h and performed at different pH values, to verify whether the performances of the material change during the reuse in different environments. The results gathered at pH 9, depicted in Fig. 7b, highlight a progressive reduction of the MB removal capacity, which was initially slow and then became marked after 5 cycles. A gradual decay of the performances was observed whatever the pH adopted, though it was relatively milder at low pH (Fig. S7). At the 7th reuse, a regeneration procedure was carried out by simply washing in water and fully drying the powders, as described in the Experimental. Consequently, in the successive batch, the MB removal capacity of the samples used in alkaline conditions was remarkably improved (90% of the initial removal efficiency was recovered at pH 9), whereas no appreciable changes were observed in the samples tested in acidic solution, namely at pH values close to the PZC of the material (see Fig. 7b and S6). The deactivation of the catalyst can be caused by several factors. The likely accumulation of strongly adsorbed dye molecules and degradation products on the surface and in the pores of the material could be partially counteracted by the regeneration treatment, useful for removing adsorbed species. In addition, a gradual modification of the surface chemistry of the hybrid titania, depending also on pH, cannot be excluded considering the involvement of dbm ligands in charge transfer complexes and the consequent possibility of their self-oxidation after prolonged processing [64].

To further investigate the long-term stability of the catalytic material under operating conditions, the second set of experiments was carried
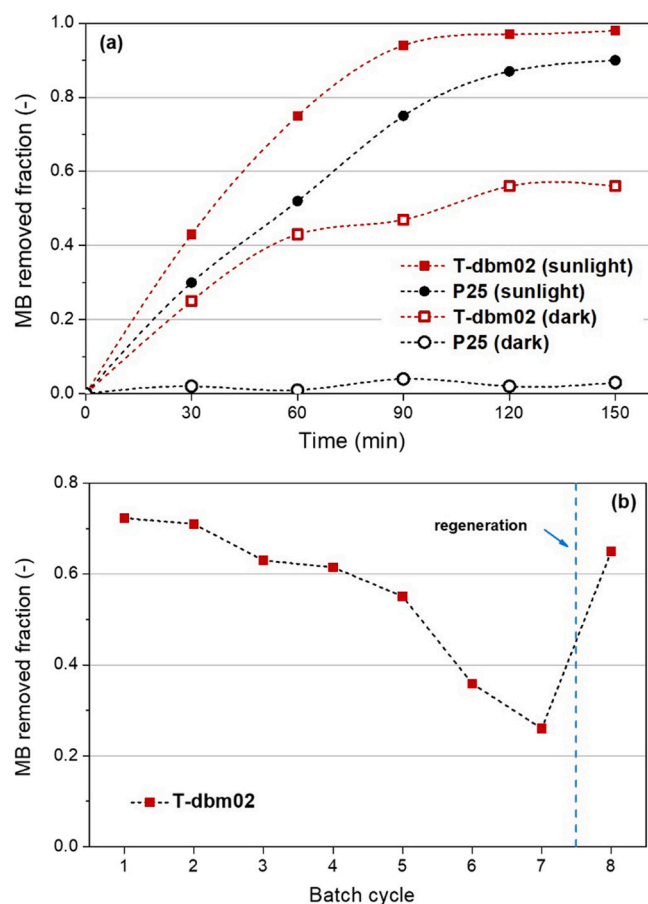
Fig. 7. (a) Effect of the sunlight exposure time on the MB removal at pH 9 on T-dbm02 and P25 TiO$_2$ as reference. (b) Repeated batches of MB sunlight-mediated removal in the presence of T-dbm02 at pH 9. After the 7th reuse, a regeneration treatment of the catalyst was performed. The dotted lines are guides for the eye.

Table 1
The pseudo-first order rate constants of the MB removal experiments reported in Fig. 7a.

Sample	Conditions	k·10^2, min^{-1}
T-dbm02	sunlight	2.31
P25	sunlight	1.43
T-dbm02	dark	0.69
P25	dark	0.02

out keeping it in water at pH 9, either exposed to sunlight, following the natural diurnal cycle, or in the dark. The samples were periodically used for a MB removal test and then stored in water again. The role of mechanical stirring of the suspension was also examined. A series of long-term runs was performed using an orbital shaker, at a relatively slow mixing speed (40 rpm). The experimental results, reported in Fig. 8a, show that, under sunlight, increasing levels of removal were obtained in the first 3 batches. In the subsequent batches, a slow reduction of dye removal was observed. It can be noted that this trend is quite different than the one previously analysed (Fig. 7a). It is tricky to interpret the initial lower activity observed in these conditions. The apparent activation of the photocatalyst in the first runs could be related to the progressive removal of some residual organics adsorbed on the xerogel surface, leading to the exposure of more active surface sites, whereas the subsequent decrease might be explained assuming that the dbm ligands undergo progressive self-degradation and depletion during long-term operation and recycling. In any case, it should be considered that in the sunlight-driven experiments the weather (hence the solar radiation intensity and continuity) is an additional variable that can cause fluctuations in the measured activity. Still, the extended storage in water allowed the removal of high fractions of MB, even after 6 cycles. The tests carried out by keeping the system in the dark showed lower MB removal efficiencies, which undergo a progressive reduction after the second batch. This is probably due to a decrease in the superoxide radical concentration, as their possible regeneration in solution from dissolved O_2 is less effective than in air. The light irradiation is supposed to play a role, even if indirect, in the process, by activating the interfacial charge transfer. When carrying out the test in the absence of titania, no significant decolouration of the solution was observed.

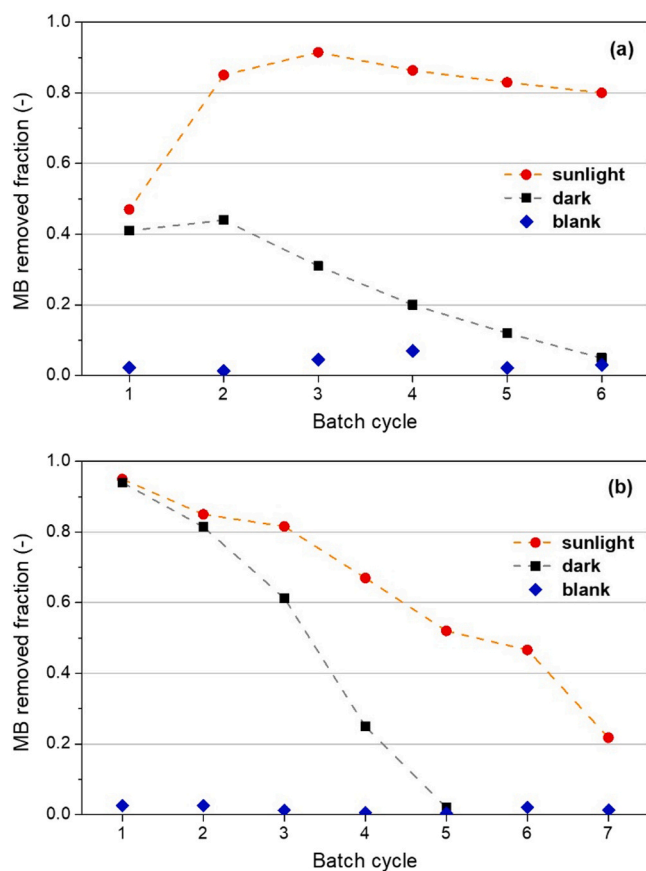A subsequent series of tests was performed using a magnetic stirrer at

Fig. 8. MB sunlight-mediated removal obtained in the presence of TiO_2-dbm at pH 9, keeping the material in water in different stirring conditions: (a) rotary shaker at 40 rpm mixer speed; (b) magnetic stirrer at 200 rpm.

a faster mixing speed (200 rpm). In this case, T-dbm02 reached a maximum MB removal capacity at the first batch, both with and without sunlight exposure (Fig. 8b). This behaviour could be explained considering that the mechanical stress due to the magnetic mixing caused a partial fragmentation of the hybrid titania microparticles, as visually observed after these experiments. Consequently, the surface/volume ratio of the particles was increased, and the surface activity was thus promoted. The fraction of MB removed after the first batch (about 95%) was comparable to the maximum value observed when using the lower-speed mixing. On the other hand, the subsequent decrease of the MB removal efficiency is faster, leading to a complete loss of activity after 6 batches under sunlight and 4 in the dark. This faster deactivation can be attributed to the acceleration of all the contributing processes, including the poisoning of the active sites and the alteration of the organic component of the hybrid catalyst. However, it is worth noting that the cumulative MB removed during 4 batches in the dark with stronger stirring is almost double than that obtained with slow mixing. When evaluating the role of mechanical stirring in the degradation process, the lately emerging concept of tribocatalysis can also be considered. It relies on the ability of some solids to harvest and use mechanical energy to promote chemical reactions, and it was recently demonstrated that even non-piezoelectric materials, such as TiO_2, can benefit from the energy input of magnetic stirring to enhance degradation processes [65]. The role of the stirring system and parameters as well as that of the reactor configuration are worth of further investigation.

3.3.4. Possible degradation mechanism over TiO_2-dbm

The results of the MB removal tests presented above clearly indicate that the disappearance of the dye in a suspension of the TiO_2-dbm particles cannot be ascribed to mere surface adsorption, since it would not be consistent with the enhanced activity under sunlight (though the adsorption on a semiconductor can be influenced by irradiation [16]) and the quite repeatable removal capacity in long-term experiments. Adsorption is indeed considered a fundamental step in heterogeneous degradation reactions, as the action of the reactive oxygen species produced at the surface of the catalyst is supposed to be exerted mainly on adsorbed substrates. MB can adsorb on solid surfaces not only by electrostatic attraction but also through hydrogen bonding, π-π electron interaction, and hydrophobic interactions [7]. Hence the functionalization of oxide surfaces is often employed to improve the adsorption, and studies on silica modification showed that the introduction of hydrophobic groups favours MB physisorption [66,67]. The TiO_2-dbm xerogel surface is negatively charged already at neutral pH (see Fig. 6) and presents both abundant hydroxyl groups (see Fig. 1) and exposed aromatic rings of the dbm molecules, which provide it with a marked hydrophobic behaviour. All these features can promote the adsorption of the dye by different kinds of interaction.

Under solar radiation, a typical photocatalytic mechanism can be envisaged to occur, as illustrated in Scheme 2: dbm acts as a photosensitizer through a direct interfacial charge transfer, enabling the absorption of a portion of visible light by the hybrid titania, and the consequent separation of electron/hole pairs. Then photogenerated holes in the valence band can produce hydroxyl ($^{\bullet}OH$) radicals from water or hydroxide ions, while photogenerated electrons in the conduction band can generate $O_2^{\bullet-}$ radicals from dissolved O_2. Both these ROS were reported to be active in the MB degradation processes, depending on the tested material and conditions, and the direct oxidation of adsorbed molecules by holes cannot be excluded [4].

On the other hand, the oxidative degradation activity observed in the absence of light, previously reported for ZrO_2-acac and TiO_2-acac hybrids, is rather uncommon. In these conditions, the stably adsorbed superoxide radicals detected by EPR (see Fig. 4) are expected to play a leading role. It is known that $O_2^{\bullet-}$ tends to be protonated to hydroperoxyl ($HO_2^{\bullet}$) radical in water solution and then to be converted into $^{\bullet}OH$ [8], as was proven to occur also in suspensions of TiO_2-acac and rosin-modified TiO_2 kept in the dark by EPR spin trapping measurements [25,26].
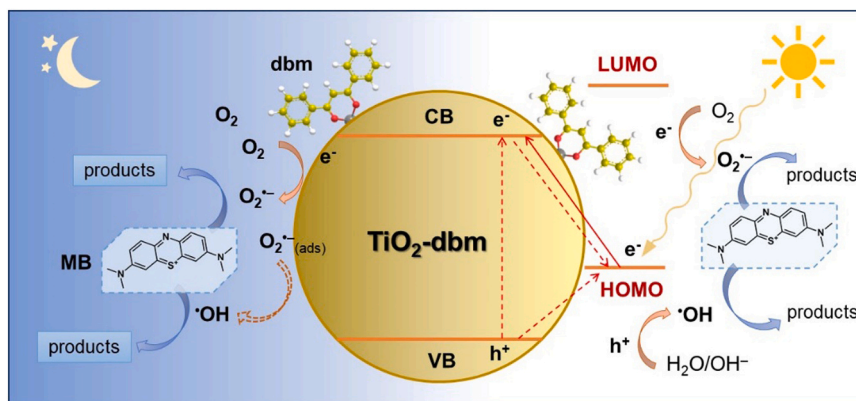
Scheme 2. Possible general mechanism of dye degradation by TiO$_2$-dbm hybrid material under solar radiation and in the darkness.

However, in a work showing that rutile-rich TiO$_2$ may preferentially produce and stabilize O$_2^{\bullet-}$ during the photocatalytic run, superoxide was proposed to be more efficient and selective in the oxidation of MB because of steric effects [68]. The prevalent role of O$_2^{\bullet-}$/HO$_2^{\bullet}$ was reported also by researchers dealing with non-irradiated TiO$_2$-H$_2$O$_2$ systems, which were found to be able to degrade MB, though less effectively than in ambient light [69,70]. It should be emphasized that the diketone-containing hybrid oxides do not need any radical source except O$_2$ for the generation of ROS. Ideally, the redox cycle could be closed by an electron donor in solution (such as an organic compound) that restores the initial electron distribution at the hybrid surface. It may be supposed that, beside carrying a certain amount of superoxide radicals adsorbed on its surface, the material is able to generate them also in water suspension, by reduction of dissolved oxygen molecules, thus sustaining the oxidative degradation during prolonged contact with water. This hypothesis is supported by a stoichiometric calculation, indicating that the number of pollutant molecules degraded in the dark tests is orders of magnitude higher than the number of adsorbed O$_2^{\bullet-}$ radicals estimated from EPR spectra, as previously reported [25]. The importance of the contact with O$_2$ on the redox activity of the material is highlighted by the observations that a simple regeneration by washing in water and drying in air can extend its utilization.

The behaviour of these hybrid materials bears some resemblance to the "photocatalytic memory" effect that has recently attracted interest in the field. It is exhibited by heterostructures with a component capable of acting as electron storage, accumulating electrons during irradiation and releasing them during the dark cycle, thus maintaining considerable activity even in a few hours of darkness [21,22]. Such "round-the-clock" photocatalytic systems were obtained also coupling TiO$_2$ with some other semiconductors and used for degradation processes [18,20]. In the studied hybrid semiconductors, the organic ligand can be seen as a source of additional charge and the surface-immobilized superoxide radicals as a kind of electron storage, however, their generation seems to be possible both under ambient light and in the absence of photoexcitation, as illustrated in Scheme 2. The development of hybrid oxide-based heterojunctions and their immobilization on suitable supports are among the possible steps to further advance the efficiency and applicability of these systems.

4. Conclusions

The coordination of titanium by dibenzoylmethane in an amorphous oxide network results in a solar photocatalyst able to trigger oxidative degradation even in the absence of light. The Ti-dbm charge transfer complex simultaneously activates visible light absorption and promotes the formation of extremely stable superoxide radicals by reduction of molecular oxygen. Higher is the organic ligand content, larger is yield of radicals, and longer their storage on the material's surface. The TiO$_2$-

dbm xerogel with a nominal dbm/Ti ratio of 0.2 exhibits a superior efficiency in the removal of methylene blue from aqueous solution compared to the reference P25 TiO$_2$ under natural sunlight (62% higher apparent rate constant). Intriguingly, it has also a considerable activity in the dark. Repeated batch tests show that in optimal conditions TiO$_2$-dbm can keep a removal efficiency above 80% for at least four consecutive cycles and recover most of the activity after a simple regeneration treatment by washing in water and drying in air. The negative surface charge at near-neutral pH makes TiO$_2$-dbm suitable for the removal of cationic contaminants, taking advantage of electrostatic interactions, while the phenyl rings exposed at the particles' surface may promote the adsorption of nonpolar organic pollutants through hydrophobic and π-π electron interactions.

The peculiar features of this hybrid semiconductor open new perspectives in the development of extremely versatile catalysts, able to work under low-intensity and intermittent light sources, such as natural sunlight, or in systems that cannot be easily illuminated (e.g., packed bed reactors). These materials may be suitable for a variety of applications, not only sustainable and energy-saving advanced oxidation processes for water remediation and treatment, but also more selective reactions that require the prevalent formation of superoxide radicals. Furthermore, these findings may inspire the design of nanomaterials for high-performing biological and medical methodologies, for example antimicrobial devices and photodynamic or chemodynamic therapy, based on the controlled generation of reactive oxygen species.

CRediT authorship contribution statement

Pirozzi Domenico: Conceptualization, Formal analysis, Methodology, Writing – review & editing. **Imparato Claudio:** Conceptualization, Formal analysis, Investigation, Writing – review & editing. **Bonifazzi Manfred Maria:** Formal analysis, Investigation. **D'Errico Gerardino:** Supervision, Writing – review & editing. **Bifulco Aurelio:** Formal analysis, Visualization. **Tammaro Olimpia:** Formal analysis, Investigation. **Esposito Serena:** Validation, Writing – review & editing. **Aronne Antonio:** Methodology, Supervision, Validation, Writing – review & editing.

Declaration of Competing Interest

The authors declare that they have no known competing financial interests or personal relationships that could have appeared to influence the work reported in this paper.

Data Availability

Data will be made available on request.

Appendix A. Supporting information

Supplementary data associated with this article can be found in the online version at doi:10.1016/j.colsurfa.2024.133148.

References

[1] R. Al-Tohamy, S.S. Ali, F. Li, K.M. Okasha, Y.A.G. Mahmoud, T. Elsamahy, H. Jiao, Y. Fu, J. Sun, A critical review on the treatment of dye-containing wastewater: ecotoxicological and health concerns of textile dyes and possible remediation approaches for environmental safety, Ecotoxicol. Environ. Saf. 231 (2022) 113160, https://doi.org/10.1016/J.ECOENV.2021.113160.

[2] C. Imparato, A. Bifulco, B. Silvestri, G. Vitiello, Recent advances in endocrine disrupting compounds degradation through metal oxide-based nanomaterials, Catalysts 12 (2022) 289, https://doi.org/10.3390/catal12030289.

[3] F. Tescione, O. Tammaro, A. Bifulco, G. Del Monaco, S. Esposito, M. Pansini, B. Silvestri, A. Costantini, Silica meets tannic acid: designing green nanoplatforms for environment preservation, Molecules 27 (2022) 1994, https://doi.org/10.3390/molecules27061944.

[4] A. Rafiq, M. Ikram, S. Ali, F. Niaz, M. Khan, Q. Khan, M. Maqbool, Photocatalytic degradation of dyes using semiconductor photocatalysts to clean industrial water pollution, J. Ind. Eng. Chem. 97 (2021) 111–128, https://doi.org/10.1016/j.jiec.2021.02.017.

[5] M. Sörengård, E. Östblom, S. Köhler, L. Ahrens, Adsorption behavior of per- and polyfluoroalkyl substances (PFASs) to 44 inorganic and organic sorbents and use of dyes as proxies for PFAS sorption, J. Environ. Chem. Eng. 8 (2020) 103744, https://doi.org/10.1016/J.JECE.2020.103744.

[6] H.M. Solayman, M.A. Hossen, A. Abd Aziz, N.Y. Yahya, K.H. Leong, L.C. Sim, M. U. Monir, K.D. Zoh, Performance evaluation of dye wastewater treatment technologies: A review, J. Environ. Chem. Eng. 11 (2023) 109610, https://doi.org/10.1016/J.JECE.2023.109610.

[7] Y. Shi, Q. Chang, T. Zhang, G. Song, Y. Sun, G. Ding, A review on selective dye adsorption by different mechanisms, J. Environ. Chem. Eng. 10 (2022) 108639, https://doi.org/10.1016/J.JECE.2022.108639.

[8] C. Dong, W. Fang, Q. Yi, J. Zhang, A comprehensive review on reactive oxygen species (ROS) in advanced oxidation processes (AOPs), Chemosphere 308 (2022) 136205, https://doi.org/10.1016/j.chemosphere.2022.136205.

[9] T. Liu, S. Xiao, N. Li, J. Chen, X. Zhou, Y. Qian, C.H. Huang, Y. Zhang, Water decontamination via nonradical process by nanoconfined Fenton-like catalysts, Nat. Commun. 14 (2023) 1–12, https://doi.org/10.1038/s41467-023-38677-1.

[10] O. Tammaro, N. Morante, A. Marocco, M. Fontana, M. Castellino, G. Barrera, P. Allia, P. Tiberto, R. Arletti, R. Fantini, V. Vaiano, S. Esposito, D. Sannino, M. Pansini, The beneficial role of nano-sized Fe$_3$O$_4$ entrapped in ultra-stable Y zeolite for the complete mineralization of phenol by heterogeneous photo-Fenton under solar light, Chemosphere 345 (2023) 140400, https://doi.org/10.1016/J.CHEMOSPHERE.2023.140400.

[11] A. Ahmadi, M. Hajilou, S. Zavari, S. Yaghmaei, A comparative review on adsorption and photocatalytic degradation of classified dyes with metal/non-metal-based modification of graphitic carbon nitride nanocomposites: Synthesis, mechanism, and affecting parameters, J. Clean. Prod. 382 (2023) 134967, https://doi.org/10.1016/J.JCLEPRO.2022.134967.

[12] M. Shaban, A.M. Ahmed, N. Shehata, M.A. Betiha, A.M. Rabie, Ni-doped and Ni/Cr co-doped TiO$_2$ nanotubes for enhancement of photocatalytic degradation of methylene blue, J. Colloid Interface Sci. 555 (2019) 31–41, https://doi.org/10.1016/J.JCIS.2019.07.070.

[13] S. Krishnan, A. Shriwastav, Application of TiO$_2$ nanoparticles sensitized with natural chlorophyll pigments as catalyst for visible light photocatalytic degradation of methylene blue, J. Environ. Chem. Eng. 9 (2021) 104699, https://doi.org/10.1016/J.JECE.2020.104699.

[14] A.S.M. Nur, M. Sultana, A. Mondal, S. Islam, F.N. Robel, A. Islam, M.S.A. Sumi, A review on the development of elemental and codoped TiO$_2$ photocatalysts for enhanced dye degradation under UV–vis irradiation, J. Water Process Eng. 47 (2022) 102728, https://doi.org/10.1016/J.JWPE.2022.102728.

[15] G. Zhang, G. Kim, W. Choi, Visible light driven photocatalysis mediated via ligand-to-metal charge transfer (LMCT): an alternative approach to solar activation of titania, Energy Environ. Sci. 7 (2014) 954–966, https://doi.org/10.1039/c3ee43147a.

[16] F. Parrino, C. De Pasquale, L. Palmisano, Influence of surface-related phenomena on mechanism, selectivity, and conversion of TiO$_2$-induced photocatalytic reactions, ChemSusChem 12 (2019) 589–602, https://doi.org/10.1002/cssc.201801898.

[17] S. Wei, X. Hu, H. Liu, Q. Wang, C. He, Rapid degradation of Congo red by molecularly imprinted polypyrrole-coated magnetic TiO$_2$ nanoparticles in dark at ambient conditions, J. Hazard. Mater. 294 (2015) 168–176, https://doi.org/10.1016/J.JHAZMAT.2015.03.067.

[18] H. Khan, M.G. Rigamonti, G.S. Patience, D.C. Boffito, Spray dried TiO$_2$/WO$_3$ heterostructure for photocatalytic applications with residual activity in the dark, Appl. Catal. B Environ. 226 (2018) 311–323, https://doi.org/10.1016/J.APCATB.2017.12.049.

[19] V. Vaiano, O. Sacco, D. Sannino, Electric energy saving in photocatalytic removal of crystal violet dye through the simultaneous use of long-persistent blue phosphors, nitrogen-doped TiO$_2$ and UV-light emitting diodes, J. Clean. Prod. 210 (2019) 1015–1021, https://doi.org/10.1016/J.JCLEPRO.2018.11.017.

[20] M.P. Ravikumar, S. Bharathkumar, B. Urupalli, M.K. Murikinati, S. M. Venkatakrishnan, S. Mohan, Insights into the photocatalytic memory effect of magneto- plasmonic Ag−Fe$_3$O$_4$@TiO$_2$ ternary nanocomposites for dye degradation and H$_2$ production under light and dark conditions, Energy Fuels 36 (2022) 11503–11514, https://doi.org/10.1021/acs.energyfuels.2c01563.

[21] T. Cai, Y. Liu, L. Wang, W. Dong, G. Zeng, Recent advances in round-the-clock photocatalytic system: Mechanisms, characterization techniques and applications, J. Photochem. Photobiol. C. Photochem. Rev. 39 (2019) 58–75, https://doi.org/10.1016/J.JPHOTOCHEMREV.2019.03.002.

[22] C. Zhang, Y. Li, M. Li, D. Shuai, X. Zhou, X. Xiong, C. Wang, Q. Hu, Continuous photocatalysis via photo-charging and dark-discharging for sustainable environmental remediation: performance, mechanism, and influencing factors, J. Hazard. Mater. 420 (2021) 126607, https://doi.org/10.1016/J.JHAZMAT.2021.126607.

[23] F. Sannino, D. Pirozzi, G. Vitiello, G. D'Errico, A. Aronne, E. Fanelli, P. Pernice, Oxidative degradation of phenanthrene in the absence of light irradiation by hybrid ZrO$_2$-acetylacetonate gel-derived catalyst, Appl. Catal. B Environ. 156–157 (2014) 101–107.

[24] F. Sannino, P. Pernice, C. Imparato, A. Aronne, G. D'Errico, L. Minieri, M. Perfetti, D. Pirozzi, Hybrid TiO$_2$-acetylacetonate amorphous gel-derived material with stably adsorbed superoxide radical active in oxidative degradation of organic pollutants, RSC Adv. 5 (2015) 93831–93839, https://doi.org/10.1039/c5ra21176j.

[25] D. Pirozzi, C. Imparato, G. D'Errico, G. Vitiello, A. Aronne, F. Sannino, Three-year lifetime and regeneration of superoxide radicals on the surface of hybrid TiO$_2$ materials exposed to air, J. Hazard. Mater. 387 (2020) 121716, https://doi.org/10.1016/j.jhazmat.2019.121716.

[26] P. Amato, M. Fantauzzi, F. Sannino, I. Ritacco, G. Santoriello, M. Farnesi, C. Imparato, A. Bifulco, G. Vitiello, L. Caporaso, A. Rossi, A. Aronne, Indirect daylight oxidative degradation of polyethylene microplastics by a bio-waste modified TiO$_2$-based material, J. Hazard. Mater. 463 (2024) 132907, https://doi.org/10.1016/j.jhazmat.2023.132907.

[27] I. Ritacco, C. Imparato, L. Falivene, L. Cavallo, A. Magistrato, L. Caporaso, M. Farnesi Camellone, A. Aronne, Spontaneous production of ultrastable reactive oxygen species on titanium oxide surfaces modified with organic ligands, Adv. Mater. Interfaces 8 (2021) 2100629, https://doi.org/10.1002/admi.202100629.

[28] L.A. Almeida, M. Habran, R.D.S. Carvalho, M.E.H.M. da Costa, M. Cremona, B. C. Silva, K. Krambrock, O.G. Pandoli, E. Morgado, B.A. Marinkovic, The influence of calcination temperature on photocatalytic activity of TiO$_2$-acetylacetone charge transfer complex towards degradation of NOx under visible light, Catalysts 10 (2020) 1463, https://doi.org/10.3390/CATAL10121463.

[29] L.A. Almeida, A. Dosen, J. Viol, B.A. Marinkovic, TiO2-acetylacetone as an efficient source of superoxide radicals under reduced power visible light: photocatalytic degradation of chlorophenol and tetracycline, Catalysts 12 (2022) 116, https://doi.org/10.3390/CATAL12020116/S1.

[30] W. Huang, X. Wang, W. Zhang, S. Zhang, Y. Tian, Z. Chen, W. Fang, J. Ma, Intraligand charge transfer boosts visible-light-driven generation of singlet oxygen by metal-organic frameworks, Appl. Catal. B Environ. 273 (2020) 119087, https://doi.org/10.1016/J.APCATB.2020.119087.

[31] Sigma-Aldrich, Dibenzoylmethane Safety Data Sheet, revised 30–04-2022, n.d.

[32] J. Zawadiak, M. Mrzyczek, Influence of substituent on UV absorption and keto–enol tautomerism equilibrium of dibenzoylmethane derivatives, Spectrochim. Acta Part A Mol. Biomol. Spectrosc. 96 (2012) 815–819, https://doi.org/10.1016/J.SAA.2012.07.109.

[33] A.T. Wagner, P.W. Roesky, Rare-earth metal oxo/hydroxo clusters – synthesis, structures, and applications, Eur. J. Inorg. Chem. 2016 (2016) 782–791, https://doi.org/10.1002/EJIC.201501281.

[34] N. Tohge, R. Ueno, F. Chiba, K. Kintaka, J. Nishii, Characteristics of diffraction gratings fabricated by the two-beam interference method using photosensitive hybrid gel films, J. Sol. -Gel Sci. Technol. 19 (2000) 119–123, https://doi.org/10.1023/A:1008786827194.

[35] H. Segawa, S. Inque, K. Watanabe, R. Ohashi, H. Nitani, M. Nomura, A study of photoreactions in photosensitive TiO$_2$ hybrid gel films induced by UV irradiation, J. Ceram. Soc. Jpn. 123 (2015) 793–799, https://doi.org/10.2109/jcersj2.123.793.

[36] M.L. Addonizio, A. Aronne, C. Imparato, Amorphous hybrid TiO$_2$ thin films: The role of organic ligands and UV irradiation, Appl. Surf. Sci. 502 (2020) 144095, https://doi.org/10.1016/j.apsusc.2019.144095.

[37] E.L. Crepaldi, G.J. Galo, D. Grosso, P.A. Albouy, C. Sanchez, Design and post-functionalisation of ordered mesoporous zirconia thin films, Chem. Commun. 1 (2001) 1582–1583, https://doi.org/10.1039/B104623N.

[38] V.G. Kessler, G.I. Spijksma, G.A. Seisenbaeva, S. Håkansson, D.H.A. Blank, H.J. M. Bouwmeester, New insight in the role of modifying ligands in the sol-gel processing of metal alkoxide precursors: a possibility to approach new classes of materials, J. Sol. -Gel Sci. Technol. 40 (2006) 163–179, https://doi.org/10.1007/s10971-006-9209-6.

[39] S. Esposito, Evolution of sol–gel chemistry, in: SpringerBriefs Mater, Springer, 2023, pp. 43–51, https://doi.org/10.1007/978-3-031-20723-5_5.

[40] G.J.A.A. Soler-Illia, E. Scolan, A. Louis, P.A. Albouy, C. Sanchez, Design of meso-structured titanium oxo based hybrid organic-inorganic networks, N. J. Chem. 25 (2001) 156–165, https://doi.org/10.1039/b006139p.

[41] A. Mancuso, N. Blangetti, O. Sacco, F.S. Freyria, B. Bonelli, S. Esposito, D. Sannino, V. Vaiano, Photocatalytic degradation of crystal violet dye under visible light by Fe-doped TiO$_2$ prepared by reverse-micelle sol–gel method, Nanomaterials 13 (2023) 270, https://doi.org/10.3390/NANO13020270.

[42] M.J. Percy, J.R. Bartlett, L. Spiccia, B.O. West, J.L. Woolfrey, Influence of β-diketones on the hydrolysis and growth of particles from zirconium(IV) n-

propoxide, J. Sol. -Gel Sci. Technol. 19 (2000) 315–319, https://doi.org/10.1023/A:1008781515324.

[43] V.G. Kessler, G.A. Seisenbaeva, Molecular mechanisms of the metal oxide sol-gel process and their application in approaches to thermodynamically challenging complex oxide materials, J. Sol. -Gel Sci. Technol. 107 (2023) 190–200, https://doi.org/10.1007/s10971-023-06120-y.

[44] C. Imparato, G. D'Errico, W. Macyk, M. Kobielusz, G. Vitiello, A. Aronne, Interfacial charge transfer complexes in TiO_2-enediol hybrids synthesized by sol-gel, Langmuir 38 (2022) 1821–1832, https://doi.org/10.1021/acs.langmuir.1c02939.

[45] S.F. Tayyari, H. Rahemi, A.R. Nekoei, M. Zahedi-Tabrizi, Y.A. Wang, Vibrational assignment and structure of dibenzoylmethane. A density functional theoretical study, Spectrochim. Acta - Part A. 66 (2007) 394–404, https://doi.org/10.1016/j.saa.2006.03.010.

[46] A.R. Nekoei, M. Vakili, M. Hakimi-Tabar, S.F. Tayyari, R. Afzali, H.G. Kjaergaard, Theoretical study, and infrared and Raman spectra of copper(II) chelated complex with dibenzoylmethane, Spectrochim. Acta - Part A Mol. Biomol. Spectrosc. 128 (2014) 272–279, https://doi.org/10.1016/j.saa.2014.02.097.

[47] I. Karlsson, L. Hillerström, A.L. Stenfeldt, J. Mårtensson, A. Börje, Photodegradation of dibenzoylmethanes: Potential cause of photocontact allergy to sunscreens, Chem. Res. Toxicol. 22 (2009) 1881–1892, https://doi.org/10.1021/TX900284E.

[48] I.O. Acik, J. Madarász, M. Krunks, K. Tõnsuaadu, G. Pokol, L. Niinistö, Titanium (IV) acetylacetonate xerogels for processing titania films: a thermoanalytical study, J. Therm. Anal. Calorim. 97 (2009) 39–45, https://doi.org/10.1007/s10973-008-9647-1.

[49] B. Bonelli, O. Tammaro, F. Martinovic, R. Nasi, G. Dell'Agli, P. Rivolo, F. Giorgis, N. Ditaranto, F.A. Deorsola, S. Esposito, Reverse micelle strategy for the synthesis of $MnOx$-TiO_2 active catalysts for NH_3-selective catalytic reduction of NOx at both low temperature and low Mn content, ACS Omega 6 (2021) 24562–24574, https://doi.org/10.1021/acsomega.1c03153.

[50] P.K. Verma, A. Steinbacher, F. Koch, P. Nuernberger, T. Brixner, Monitoring ultrafast intramolecular proton transfer processes in an unsymmetric β-diketone, Phys. Chem. Chem. Phys. 17 (2015) 8459–8466, https://doi.org/10.1039/C4CP05811A.

[51] K.L. Antcliff, D.M. Murphy, E. Griffiths, E. Giamello, The interaction of H_2O_2 with exchanged titanium oxide systems (TS-1, TiO_2, [Ti]-APO-5, Ti-ZSM-5), Phys. Chem. Chem. Phys. 5 (2003) 4306–4316, https://doi.org/10.1039/b306398b.

[52] S. Heinrich, M. Plettig, E. Klemm, Role of the Ti(IV)-superoxide species in the selective oxidation of alkanes with hydrogen peroxide in the gas phase on titanium silicalite-1: an in situ EPR investigation, Catal. Lett. 141 (2011) 251–258, https://doi.org/10.1007/s10562-010-0534-6.

[53] X. Zhang, Z. Li, B. Zeng, C. Li, H. Han, EPR study of charge separation associated states and reversibility of surface bound superoxide radicals in $SrTiO_3$ photocatalyst, J. Energy Chem. 70 (2022) 388–393, https://doi.org/10.1016/J.JECHEM.2022.02.038.

[54] C.O. Amor, K. Elghniji, Improving charge separation, photocurrent and photocatalytic activities of Dy-doped TiO_2 by surface modification with salicylic acid, J. Mater. Sci. Mater. Electron. (2020), https://doi.org/10.1007/s10854-020-04606-x.

[55] G. Chianese, I. Fasolino, C. Tramontano, L. De Stefano, C. Imparato, A. Aronne, L. Ambrosio, M.G. Raucci, I. Rea, ROS-generating hyaluronic acid-modified zirconium dioxide-acetylacetonate nanoparticles as a theranostic platform for the treatment of osteosarcoma, Nanomaterials 13 (2023) 54, https://doi.org/10.3390/nano13010054.

[56] R.J. Bleicher, D.D. Kloth, D. Robinson, P. Axelrod, Inflammatory cutaneous adverse effects of methylene blue dye injection for lymphatic mapping/sentinel lymphadenectomy, J. Surg. Oncol. 99 (2009) 356–360, https://doi.org/10.1002/JSO.21240.

[57] S. Rajagopal, B. Paramasivam, K. Muniyasamy, Photocatalytic removal of cationic and anionic dyes in the textile wastewater by H_2O_2 assisted TiO_2 and micro-cellulose composites, Sep. Purif. Technol. 252 (2020) 117444, https://doi.org/10.1016/J.SEPPUR.2020.117444.

[58] J.J. Salazar-Rabago, R. Leyva-Ramos, J. Rivera-Utrilla, R. Ocampo-Perez, F. J. Cerino-Cordova, Biosorption mechanism of Methylene Blue from aqueous solution onto White Pine (Pinus durangensis) sawdust: effect of operating conditions, Sustain. Environ. Res. 27 (2017) 32–40, https://doi.org/10.1016/J.SERJ.2016.11.009.

[59] D.L. Liao, G.S. Wu, B.Q. Liao, Zeta potential of shape-controlled TiO_2 nanoparticles with surfactants, Colloids Surf. A Physicochem. Eng. Asp. 348 (2009) 270–275, https://doi.org/10.1016/J.COLSURFA.2009.07.036.

[60] P.K. Dutta, A.K. Ray, V.K. Sharma, F.J. Millero, Adsorption of arsenate and arsenite on titanium dioxide suspensions, J. Colloid Interface Sci. 278 (2004) 270–275, https://doi.org/10.1016/J.JCIS.2004.06.015.

[61] Z. Cao, T. Zhang, P. Ren, D. Cao, Y. Lin, L. Wang, B. Zhang, X. Xiang, Doping of chlorine from a neoprene adhesive enhances degradation efficiency of dyes by structured TiO_2-coated photocatalytic fabrics, Catalysts 10 (2020) 69, https://doi.org/10.3390/catal10010069.

[62] B.M. Saalidong, S.A. Aram, S. Otu, P.O. Lartey, Examining the dynamics of the relationship between water pH and other water quality parameters in ground and surface water systems, PLoS One 17 (2022) e0262117, https://doi.org/10.1371/JOURNAL.PONE.0262117.

[63] J. Passaro, C. Imparato, D. Parida, A. Bifulco, F. Branda, A. Aronne, Electrospinning of PVP-based ternary composites containing SiO_2 nanoparticles and hybrid TiO_2 microparticles with adsorbed superoxide radicals, Compos. Part B Eng. 238 (2022) 109874, https://doi.org/10.1016/j.compositesb.2022.109874.

[64] K. Qi, F. Zasada, W. Piskorz, P. Indyka, J. Gryboś, M. Trochowski, M. Buchalska, M. Kobielusz, W. Macyk, Z. Sojka, Self-sensitized photocatalytic degradation of colorless organic pollutants attached to rutile nanorods: experimental and theoretical DFT+D studies, J. Phys. Chem. C. 120 (2016) 5442–5456, https://doi.org/10.1021/acs.jpcc.5b10983.

[65] X. Cui, P. Li, H. Lei, C. Tu, D. Wang, Z. Wang, W. Chen, Greatly enhanced tribocatalytic degradation of organic pollutants by TiO_2 nanoparticles through efficiently harvesting mechanical energy, Sep. Purif. Technol. 289 (2022) 120814, https://doi.org/10.1016/J.SEPPUR.2022.120814.

[66] D. Parida, K.A. Salmeia, A. Sadeghpour, S. Zhao, A.K. Maurya, K.I. Assaf, E. Moreau, R. Pauer, S. Lehner, M. Jovic, H. Cordula, S. Gaan, Template-free synthesis of hybrid silica nanoparticle with functionalized mesostructure for efficient methylene blue removal, Mater. Des. 201 (2021) 109494, https://doi.org/10.1016/j.matdes.2021.109494.

[67] H. Han, W. Wei, Z. Jiang, J. Lu, J. Zhu, J. Xie, Removal of cationic dyes from aqueous solution by adsorption onto hydrophobic/hydrophilic silica aerogel, Colloids Surf. A Physicochem. Eng. Asp. 509 (2016) 539–549, https://doi.org/10.1016/J.COLSURFA.2016.09.056.

[68] Z. Ma, Q. Jia, C. Tao, B. Han, Highlighting unique function of immobilized superoxide on TiO_2 for selective photocatalytic degradation, Sep. Purif. Technol. 238 (2020) 116402, https://doi.org/10.1016/j.seppur.2019.116402.

[69] L.D. Sánchez, S.F.M. Taxt-Lamolle, E.O. Hole, A. Krivokapić, E. Sagstuen, H. J. Haugen, TiO_2 suspension exposed to H_2O_2 in ambient light or darkness: degradation of methylene blue and EPR evidence for radical oxygen species, Appl. Catal. B Environ. 142–143 (2013) 662–667, https://doi.org/10.1016/j.apcatb.2013.05.017.

[70] D. Wiedmer, E. Sagstuen, K. Welch, H.J. Haugen, H. Tiainen, Oxidative power of aqueous non-irradiated TiO_2-H_2O_2 suspensions: Methylene blue degradation and the role of reactive oxygen species, Appl. Catal. B Environ. 198 (2016) 9–15, https://doi.org/10.1016/j.apcatb.2016.05.036.